

# Strength of Three New Types of Composite Beams

A. A. TOPRAC

ALTHOUGH COMPOSITE construction is not new, having been in use in this country since the late 1930's, it owes its current popularity in building construction to relatively recent developments. Since the advantages of composite construction—reduced weight of steel, smaller live load deflection, or decreased depth of members—are most pronounced in long spans and for heavy loads, most of the early work was done in the bridge field. However, neither the original nor the revised provisions on composite construction in the specifications of the American Association of State Highway Officials (AASHO)<sup>1</sup>, which were written specifically for bridges, were directly applicable to building construction because of the different nature of the problems involved.

The 1961 and 1963 revisions of the American Institute of Steel Construction (AISC) Specification<sup>2</sup> stimulated composite design for buildings by including provisions for composite beams without encasement as well as the old requirements of 1946 for fully encased beams. Until 1961 there was no applicable specification which included the practical and proven developments of that time. The sections of the above specification dealing with this subject are based on the recommendations of the ASCE-ACI Joint Committee published in 1960<sup>3</sup> and an experimental investigation completed at Lehigh University in 1961.<sup>4, 5</sup>

The development of the headed stud shear connector in the 1950's has accelerated the acceptance of composite construction by alleviating many of the fabrication and handling problems inherent with older types of shear connectors such as the channel and the spiral.<sup>6</sup>

The 1963 AISC Specification allows the use of high strength steels conforming to American Society for Testing and Materials (ASTM) Specifications A242, A440 and A441. The yield requirements for the three high strength grades are the same, and decrease from 50,000 to 42,000 psi as the thickness of the material increases. In practice, construction steels with yield strengths up to

100,000 psi are available. The strongest are the quenched and tempered alloy steels having yield strengths in the range of 90,000 to 100,000 psi. These constructional alloy steels are covered by ASTM A514 Specification.

In traditional steel framing, particularly for building construction, deflection and/or buckling considerations often limit the application of higher strength steels. In composite construction these limitations are minimized or reduced and full advantage may be taken of the higher strength steels. In a recent study of hybrid steel girders<sup>7</sup> composed of constructional alloy steel flanges and A36 steel web, the authors state:

Both the lateral buckling problem and the deflection problem encountered through the use of high-strength steel flanges can be resolved by using composite construction. The use of this method of construction not only furnishes lateral support for the compression flange, but also increases the moment of inertia of the section so that it will not deflect as much. Since the stress in the compression flange of a composite section is usually quite low, this flange would not need to be composed of high strength steel. The use of composite construction seems to offer the most possibilities for the efficient use of high strength steel and carbon steel combinations.

## TEST PROGRAM

The investigation reported in this paper was a pilot study into three relatively unexplored areas of composite design in steel and concrete. The three areas were: (a) the use of raised patterned floor plate as a shear transfer device, (b) composite hybrid steel sections with high strength bottom flanges, and (c) composite beams with inverted steel T sections (top steel flange omitted). The purpose of the investigation was to obtain data on the structural behavior of the three types of beams subjected to static loading.

In order to achieve the above-mentioned objective, a test program of seventeen beams was designed as outlined in Table 1. There were four groups of specimens, called Series 1 to 4. For each series, the object of the investigation, the steel profile, the types of steel used and the designations of specimens are shown in Table 1.

---

*A. A. Toprac is Professor of Civil Engineering, The University of Texas, Austin, Tex., and is a Professional Member of AISC.*

---

**Table 1. Outline of Experimental Program**

Series Number	Object of Investigation	Steel Sections				Specimens
		Profile	Types of Steel <sup>b</sup>			
			Top Flange	Web	Bottom Flange	
1	Floor plate for top flange	Unsymmetrical I	Floor Pl.	A36	A36	12, 14a, 14b, 15 11 13
		Unsymmetrical I	A36	A36	A36	
		Symmetrical I	Floor Pl.	A36	A36	
2	Hybrid steel section	Symmetrical I	A36	A36	A36	21 22a, 22b, 23
		Symmetrical I	A36	A36	H.S.S. <sup>a</sup>	
3	Hybrid steel section	Symmetrical I	A36	A36, H.S.S. <sup>a</sup>	H.S.S. <sup>a</sup>	32, 33a, 33b, 34, 35
4	Steel section without top flange	Inverted tee	None	A36	A36	41a, 41b

<sup>a</sup> H.S.S. = High strength steel, either A441 or A514.

<sup>b</sup> Cross-sectional area of the steel section was the same in all specimens.

**Table 1a. Static Yield Strength of Steel Plates**

Type of Material	Plate Thickness, in.	Average Static Yield Points, ksi
A36	1/2	33.4; 33.0
A36	1/4	35.2
Floor Pl.	1/2	42.7
A441	1/2	53.0
A441	1/4	51.2
A514	1/2	110.6
A514	1/4	106 <sup>a</sup>

<sup>a</sup> For Beam 35 the lower web plate yield strength of 150 ksi is not included in this average.

The cross-sections of the specimens and the loading arrangement are shown in Fig. 1. All specimens were designed to have the same depth of steel section, concrete flange, area of steel, and thickness of flange and web plates, and were tested with the same loading arrangement.

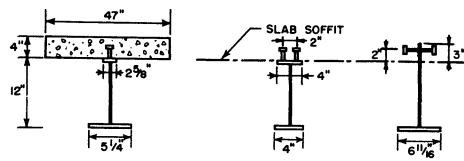
The steel sections were fabricated from A36, A441, A514 and floor steel plates; the combinations of materials used are shown in Fig. 2. The average static yield points for the steel used in the beams are shown in Table 1a. The slabs were made with river gravel and sand concrete having average cylinder strengths of 3,840 psi. They were reinforced with 0.2 percent of longitudinal steel and 0.62 percent of transverse steel. The steel sections and the concrete slabs were interconnected with headed stud shear connectors of 1/2 or 3/8-in. diameter. The number, size and spacing of studs used in each beam are given in Table 2. The last column in Table 2 compares the furnished shear connectors with those that would be required by the AISC Specification.<sup>2</sup>

The load was applied in steps of varying magnitude in such a manner that the deflections of the specimen were never allowed to decrease. All tests were continued past the ultimate load and were usually discontinued after the load had dropped off substantially from the ultimate. Deflection and end slip between the steel section and the concrete slab were measured at every load increment in all tests. In addition, strain measurements were made in the shear span and at the center line of beams 32 and 33b by means of electric resistance strain gages.

Further details on specimens, materials, and testing procedures are given in Part II of Reference 8.

**NOMENCLATURE**

- a* = depth of concrete stress block
- b* = width of concrete compression flange
- C* = total compressive force in the composite section
- c'* = compressive force in concrete flange of a composite beam with inadequate shear connectors
- c''* = compressive force in the steel section of a composite beam with inadequate shear connectors
- d* = total depth of composite section
- e* = moment arm between resultant compression and tension forces at  $M_u$
- $f'_c$  = cylinder strength of concrete at the age of testing
- $f_y$  = static yield point of steel
- M* = applied moment = 3.25 × P
- $M_m$  = maximum applied moment (includes dead load of 7.1 ft-kips)
- $M_p$  = theoretical plastic moment capacity of the steel section alone
- $M_{ps}$  = total theoretical ultimate resisting moment of the concrete slab and steel section acting together but without composite action
- $M_u$  = theoretical ultimate moment of a composite section with adequate shear connectors



NOTE: CROSS SECTION DETAILS  
 AREA OF STEEL (CONSTANT) = 6.75 in<sup>2</sup>  
 THICKNESS OF FLANGE (CONSTANT) = 0.5"  
 THICKNESS OF WEBS (CONSTANT) = 0.25"

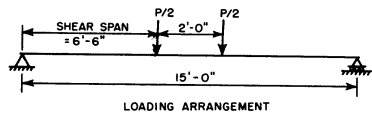


Fig. 1. Description of specimens and tests

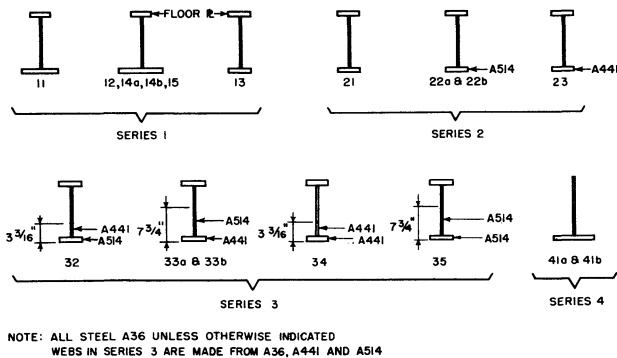


Fig. 2. Steel sections

$M_u'$  = theoretical ultimate moment of a composite section with inadequate shear connectors  
 $M_y$  = theoretical yield moment of a composite section based on first yield at any point in the beam  
 $P$  = externally applied load  
 $q_u$  = the ultimate shear strength of a shear connector  
 $T$  = total tensile force in the composite section

### TEST RESULTS AND DISCUSSION

The general modes of failure observed during the testing of composite beams of this program are discussed below. The structural behavior of each beam is presented and maximum carrying capacities, deflections and slips are given. Where applicable, comparisons are made between beams and between series. The test data and certain additional analytical studies are presented in Part II of Reference 8.

**General Modes of Failure**—All beams in this test program failed in one of three modes which will be described as: (1) flexural failure, (2) shear failure in the studs and (3) shear failure in the concrete slab.

Flexural failure of a composite section occurs when the slab compressive stresses are brought to the ultimate by bending, resulting in crushing of the concrete followed by a major loss of moment capacity. Figure 3 is a photograph of such a concrete failure in specimen 22a. Similar failure is shown in Fig. 4, which is a photograph of specimen 12 taken after it was removed from the testing machine. This type of failure implies that the shear connection was adequate. For the specimens of this

Table 2. Shear Connectors

Specimen Number <sup>a</sup>	Size of Shear Connectors	No. of Connectors per Shear Span <sup>b</sup>	Spacing of Connectors in Shear Span, in.	Percent of AISC Requirements
11	1/2 in. dia. × 3 in.	24	3 1/4	100
12	"	16	4 3/4	67
13	"	7	10	29
14a	"	7	10	29
14b	"	7	10	29
15	"	4	20	17
21	1/2 in. dia. × 3 in.	24	6 1/2	100
22a	"	26	6	72
22b	"	26	6	72
23	"	36	4 1/4	138
32	1/2 in. dia. × 3 in.	28	5 1/2	74
33a	"	48	4	126
33b	"	48	4	126
34	"	28	5 1/2	100
35	"	48	4	100
41a	3/8 in. dia. × 3 in.	58	2 3/4	—
41b	"	58	2 3/4	—

<sup>a</sup> Letters a and b distinguish between two duplicate specimens.

<sup>b</sup> In addition to the studs in the two shear spans, two studs were placed at or near the midspan of each beam.

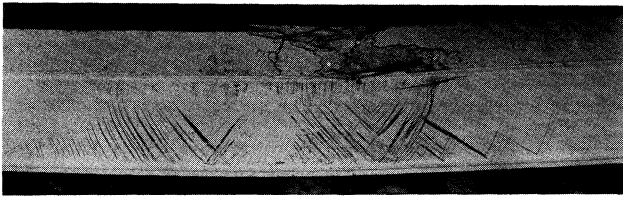


Fig. 3. Picture of Beam 22a at the end of the test. Note the crushing of the concrete slab (flexural failure). The whole steel section was yielded in tension just before the concrete crushed. The typical compression type yield lines at the upper part of the web occurred after the crushing of the concrete when the beam started carrying loads independently.

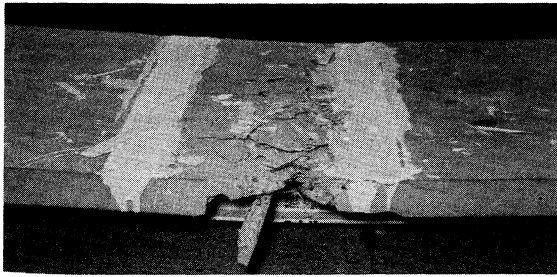


Fig. 4. Beam 12 after removal from testing machine. Photo shows typical top view of specimens which failed in flexure.

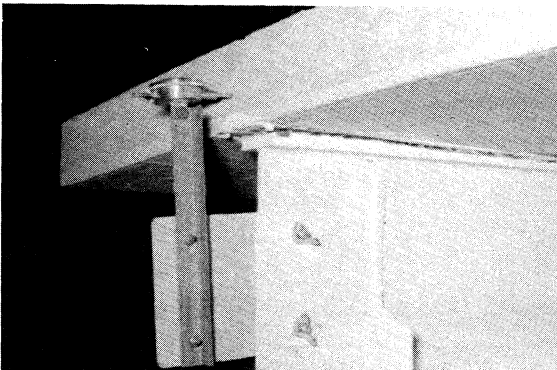


Fig. 5. Beam 14b at failure. Note the large slip between the steel flange and the concrete slab. Also the separation between steel and concrete can be clearly seen.

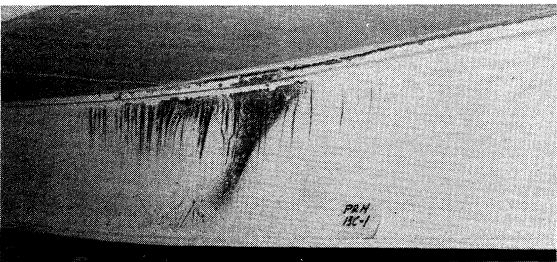


Fig. 6. View of Beam 14b before removal from testing machine. Note the slip and separation between steel shape and concrete slab. The deep compression-type yield lines occurred after the shear failure took place and the steel beam flange buckled laterally while the web buckled locally. The absence of tension yield lines above the middle of the web is apparent. The beam did not reach its calculated  $M_u$ .

program, in which the neutral axis was well above the steel section at ultimate moment, flexural failure was similar to the tension failure of an under-reinforced concrete beam. As yielding of the steel section progressed, the neutral axis rose until the compression stresses in the extreme fibers of the concrete became critical. This is the most desirable mode of failure for steel-concrete beams, since it allows the cross-section to mobilize all of its resistance and failure occurs only after considerable deflection and cracking.

Most of the beams tested in this program, following a flexural failure at their maximum moment value, were able to maintain moments which were of higher magnitude than the plastic moment value  $M_p$  of the steel section alone. This indicated that part of the concrete slab, although considerably damaged, was still available to help carry the loads, or that the strains in the steel section reached strain hardening at places where the slab was ineffective. Most of the beams exhibited remarkable reserve strength after the crushing of the concrete flange. The post-failure strength was limited by buckling of the steel section. Following the flexural failure of the composite section, the concrete slab could not provide effective lateral support in the constant moment region. Thus the steel section usually buckled either laterally or in the web.

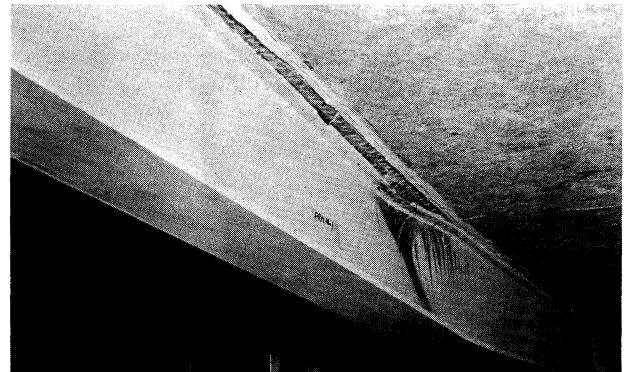


Fig. 7. View of the underside of Beam 15 which clearly shows: (a) the absence of tension type yield lines, (b) the separation between steel and concrete (c) the flange and web buckling with the accompanying compression yielding.



Fig. 8. View of Beam 32 at the end of the test. The separation at the right end and the absence of concrete crushing at midspan can be noted. This is a typical view of specimens with shear failure. The A514 portion of the web shows no yield lines. Web buckled after the maximum load was reached. Yielding due to buckling can also be seen.

Shear failure of a composite beam occurred when the shear connection was inadequate. Specimens which failed in this manner sheared off all studs in one of the shear spans and allowed the slab to separate and slip grossly, thus resulting in a major decrease in moment resistance due to the loss of composite action. After failure of the studs, the slab cracked transversely just outside one of the loads. At this point, with the studs broken, there was only friction available to provide lateral support and the steel section was relatively free to buckle. For all specimens which exhibited shear failure, the steel section was able to develop moment close to its  $M_p$  value before buckling caused the test to be stopped. Figures 5, 6, 7 and 8 are photographs which show failures of this type in specimens 14b, 15, and 32. The separation of steel and concrete is visible in all these pictures.

Only one beam, 41a, suffered a shear failure in the concrete slab. This particular beam failure will be discussed in greater detail with the results of Series 4.

**Series 1**—The objective of this series was to determine whether the use of the raised pattern floor plate for the top flange would permit a decrease in the required number of connectors. It can be seen in Table 2 that only Beam 11 had the number of connectors required by the AISC Specification<sup>2</sup> and that the number decreased in the following order: 11, 12, 14 and 15. Beam 13 had the same number of connectors as Beam 14 but it had a different shape of the steel section (Fig. 2).

Deflections and slips for all beams of this group are shown in Figs. 9 and 10 as functions of the ratio of applied moment  $M$  to the theoretical ultimate moment  $M_u$ . Table 3 gives the observed ultimate moment  $M_m$  and slip at failure. The same table also gives the theoretical values for the yield moment  $M_y$ , and the theoretical ultimate moments for composite beam with adequate shear connection  $M_u$ , for composite beam with inadequate shear connection  $M_u'$ , and for non-composite beam  $M_{ps}$ . In Table 4 comparisons are made between observed and theoretical ultimate moments.

Beams 11 and 12 failed in flexure after considerable deformation, indicating good plastic action. Beams 13, 14a, 14b and 15 failed in shear after relatively small amounts of plastic deformation and failed to develop the theoretical ultimate moment  $M_u$ . Comparisons in Figs. 9 and 10 show that the ultimate load and the deflection at ultimate load decreased with decreasing number of connectors, and the end slip at ultimate load increased rapidly as the number of shear connectors was decreased.

It is apparent from the ratios  $M_m/M_u$  in Table 4 that, as far as the ultimate strength is concerned, the floor plate did not replace effectively the connectors omitted from specimens 12 through 15. The questions then remain whether the floor plate contributed at all to the ultimate strength of the beams and whether it altered the behavior at working loads.

The ultimate moment  $M_u$  was computed on the assumption, shown in Fig. 11b, that the connection is adequate. For beams with fewer than the adequate number

Table 3. Summary of Beam Test Results

Specimen Number	Type of Failure	$M_m$ ft-kips	Theoretical Values				End slip at failure, in.
			$M_u$ ft-kips	$M_u'$ ft-kips	$M_y$ ft-kips	$M_{ps}$ ft-kips	
11	Flexure	217.7	194.5	—	142.5	83.2	0.0787
12	Flexure	207.3	198.7	188.0	142.5	90.9	0.0900
13	Shear	169.6	182.5	140.0	119.5	95.4	0.1332
14a	Shear	161.5	203.0	154.0	142.5	90.9	0.1582
14b	Shear	172.2	198.2	153.0	142.5	90.9	0.1305
15	Shear	139.1	198.0	130.5	142.5	90.9	0.1954
21	Flexure	177.7	159.6	—	119.5	86.7	0.0400
22a	Flexure	364.6	334.0	—	133.3	113.4	0.1504
22b	Flexure	364.6	342.0	—	133.3	113.4	0.1320
23	Flexure	244.3	212.0	—	133.3	104.4	0.0305
32	Shear	395.8	369.0	—	173.5	118.4	0.1710
33a	Flexure	361.3	331.0	—	184.5	123.9	0.0271
33b	Flexure	367.8	334.0	—	184.5	123.9	0.0200
34	Flexure	253.1	214.1	—	137.1	115.2	0.0650
35	Flexure	521.1	487.5	—	314.0	177.5	0.0492
41a	<sup>a</sup>	251.5	229.0	—	170.6	73.7	0.0115
41b	Flexure	234.6	215.0	—	170.6	73.7	0.0048

<sup>a</sup> Concrete shear failure

of connectors attached to a smooth top flange, the ultimate strength of the beam is governed by the aggregate strength of the connectors.<sup>9</sup> The stress distribution for such a beam with inadequate connectors is shown in Fig. 11c. Assuming that the ultimate strength of the individual studs was 12.1 kips,<sup>9</sup> the corresponding moment  $M_u'$  was computed for Beams 12 through 15 and compared with the test moment in the last column of Table 4.

The test moment  $M_m$  exceeded the computed moment  $M_u'$  in every case. However, except in Beam 13, the ratio  $M_m/M_u'$  was of the same order of magnitude as the ratio  $M_m/M_u$  for Beam 11. Thus, no contribution of the floor plate to the strength of Beams 12, 14 and 15 has been demonstrated. On the other hand, Beam 13 was stronger than indicated by the theoretical moment  $M_u'$ , suggesting that the wider floor plate of this specimen was effective in increasing the strength of the beam.

The effect of the floor plate on deformations at working load level may be estimated qualitatively from Figs. 9 and 10. It can be seen that while the end slips in Beams 12 through 15 exceeded those measured in Beam 11 even at loads of the order of  $M/M_u = 0.4$ , these increased slips did not result in increased deflections. For example, at the moment level of  $0.5 M_u$ , which has been suggested as the working moment,<sup>9</sup> the deflection of all specimens was about 0.3 in. Because of the small number of connectors in specimens 13 through 15, these results suggest strongly that the floor plate effectively increased the degree of interaction at working load level.

**Table 4. Comparison of Test Results with  $M_u$  and  $M_u'$**

Specimen Number	Type of Failure	$M_m/M_u$	$M_m/M_u'$
11	Flexure	1.118	—
12	Flexure	1.041	1.102
13	Shear	0.928	1.210
14a	Shear	0.795	1.050
14b	Shear	0.868	1.125
15	Shear	0.702	1.065
21	Flexure	1.112	—
22a	Flexure	1.110	—
22b	Flexure	1.065	—
23	Flexure	1.152	—
32	Shear	1.072	—
33a	Flexure	1.092	—
33b	Flexure	1.103	—
34	Flexure	1.180	—
35	Flexure	1.070	—
41a	<sup>a</sup>	1.098	—
41b	Flexure	1.092	—

<sup>a</sup> Concrete shear failure.

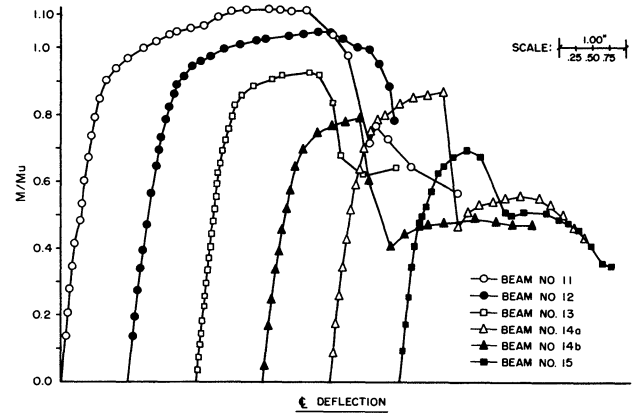


Fig. 9. Plot of  $M/M_u$  vs. centerline deflection for Series 1 beams

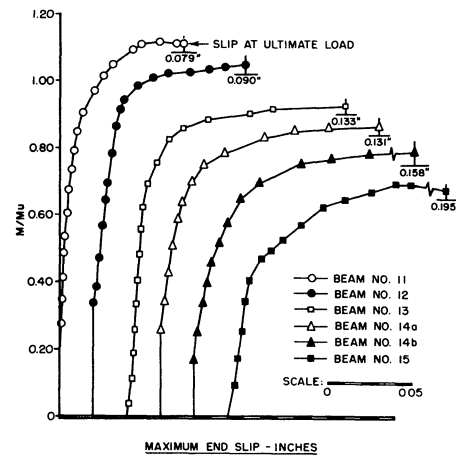


Fig. 10. Plot of  $M/M_u$  vs. maximum end slip for Series 1

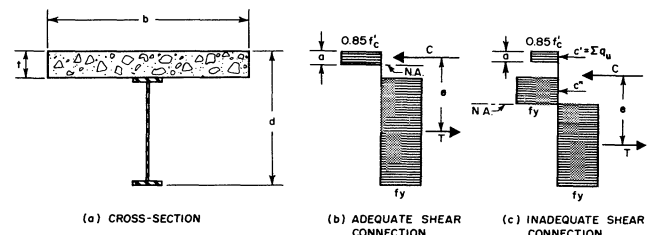


Fig. 11. Stress distribution at ultimate moment for beams with steel section of one yield strength

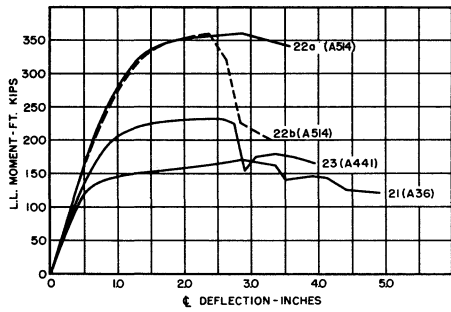


Fig. 12. Series 2, experimental moment-deflection curves

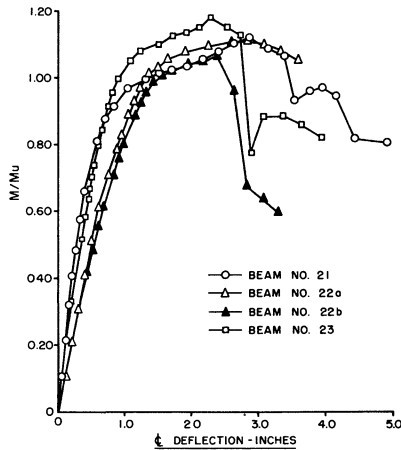


Fig. 13. Plot of  $M/M_u$  vs. centerline deflection for Series 2

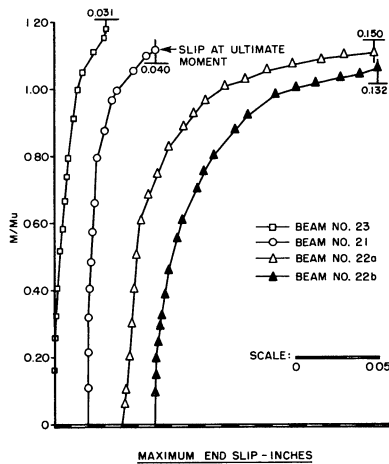


Fig. 14. Plot of  $M/M_u$  vs. maximum end slip for Series 2

**Series 2**—The objective of this series was to study the structural behavior of composite beams with hybrid steel sections. The top flange and the web in all beams was of A36 steel, but the bottom flange was of A36, A441 or A514.

The experimental moment-deflection curves for the four beams are shown in Fig. 12. It is apparent that the ultimate strength increased and the deflection at ultimate load tended to decrease with increasing strength of the bottom flange.

All four beams failed in flexure and developed the theoretical ultimate moment (Table 3). The ratio of the test to theoretical ultimate moment  $M_m/M_u$  was always in excess of 1.0 (Table 4), but the excess was the lowest for Beams 22a and 22b having only 72 percent of connectors required by the AISC Specification<sup>2</sup>, and the largest for Beam 23 having 138 percent of the required minimum number.

It is noteworthy that the stiffness at working load levels (Fig. 12) was about the same for all beams. The absolute deflection at working load level was, of course, higher in the stronger beams (Fig. 13). But the load deflection curves were essentially straight even at moments in excess of  $0.5 M_u$ . Thus the connectors were adequate both from the standpoint of strength and the standpoint of beam stiffness.

The magnitude of end slip at failure in Beams 22a and 22b (Fig. 14) indicated that the failure of the connectors in these beams was imminent.

**Series 3**—The objective of this series was to study the structural behavior of composite beams with hybrid steel sections having high strength steel not only in the bottom flange but also in the lower part of the web, and to compare the behavior of such beams with the corresponding beams of Series 2. In Beam 32, the bottom flange was of A514 steel and the lower part of the web was of A441 steel. In Beams 33a and 33b, the bottom flange was of A441 steel and the lower part of the web was of A514 steel. In Beams 34 and 35 the bottom flange and the lower part of the web were of identical steel: A441 in Beam 34 and A514 in Beam 35, as shown in Fig. 2.

All five beams developed the theoretical ultimate moment  $M_u$  of the composite section (Table 3) and, except for Beam 32, failed in flexure. Beam 32, having 74 percent of the connectors required by the AISC Specification, failed in shear at an end slip of 0.171 in. (Fig. 15) at a load exceeding the theoretical ultimate moment.

The balanced failure of Beam 32 permits calculation of the ultimate strength of the  $\frac{1}{2}$ -in. studs. At flexural

failure, the steel section had yielded through the full depth. Thus the horizontal force acting on the connectors in one shear span is equal to the area of the steel section times the yield point. In Beam 32 the average shear load per connector at failure was 14.6 kips. In Beams 22a and 22b, for which the magnitude of slips indicated that failure of connectors was imminent, the average loads per connector computed as outlined above were 14.6 and 14.4 kips, respectively.

The flexural failures of Beams 33a, 33b and 35 occurred suddenly and with little warning (Fig. 16). The sudden failure was probably caused by the fact that a relatively large depth of the slab was subjected to high compressive stresses.

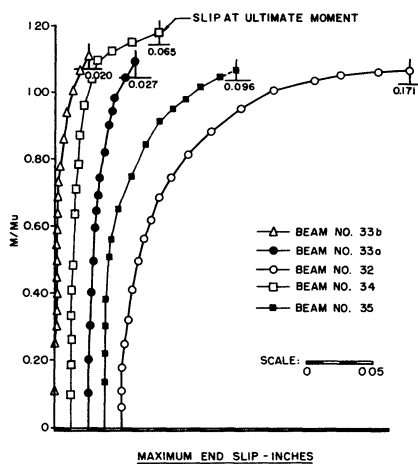


Fig. 15. Plot of  $M/M_u$  vs. maximum end slip for Series 3

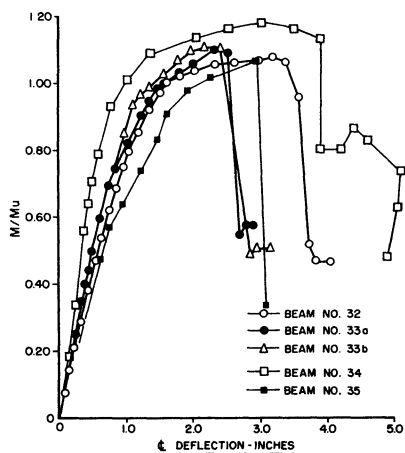


Fig. 16. Plot of  $M/M_u$  vs. centerline deflection for Series 3

The effect of the presence of high strength steel in the web is illustrated by the moment-deflection curves in Fig. 17. In this figure the type of steel used in the lower web is given in parenthesis. It is apparent that while the comparable beams of Series 2 had lower ultimate strength because of the weaker web, their stiffness in the range of working loads was essentially the same as the stiffness of Series 3 beams. The slight increase in stiffness in the elastic range for Beam 35 is due to dimensional differences. The plate thicknesses for this beam were larger than the thicknesses of the other beams. Further, the relatively larger capacity for Beam 35 is due to the unusually high yield strength of the A514 steel plate in the web.

Particularly interesting is a comparison between Beams 23 and 34. The A441 steel in the web of Beam 34 extended far enough so that the current AISC Specification<sup>2</sup> would permit the full design stress of 33 ksi to be used in the bottom flange of this beam. The absence of the A441 steel in the web of Beam 23 would require that the design stress for the flange of this beam be reduced to 24 ksi, a decrease of 28.2 percent. Yet the ultimate test moment of Beam 23 was only 3.5 percent less than that of Beam 34, and the deflections of the two beams were practically identical in the working load range.

**Series 4**—The objective of this series was to observe the behavior of a composite beam with the steel section in the shape of an inverted T. The two specimens of this series were of the same design.

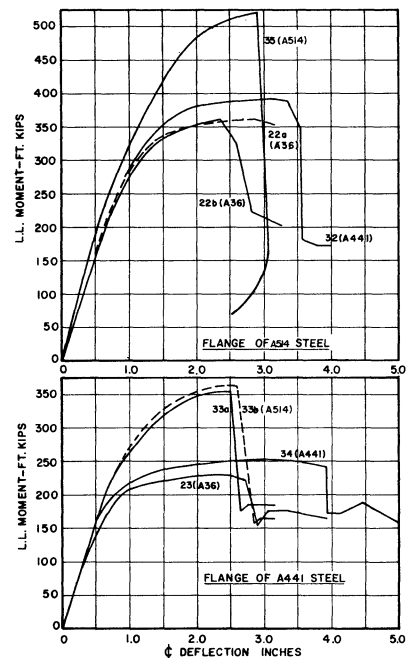


Fig. 17. Comparisons between Series 2 and 3 beams

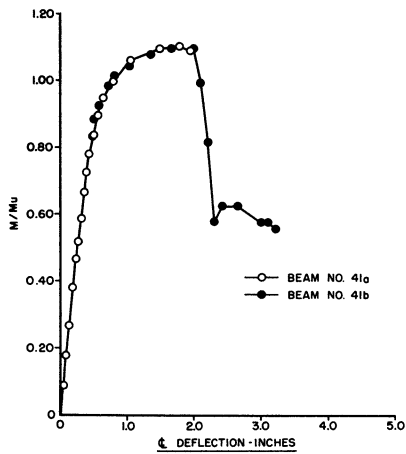


Fig. 18. Plot of  $M/M_u$  vs. centerline deflection for Series 4

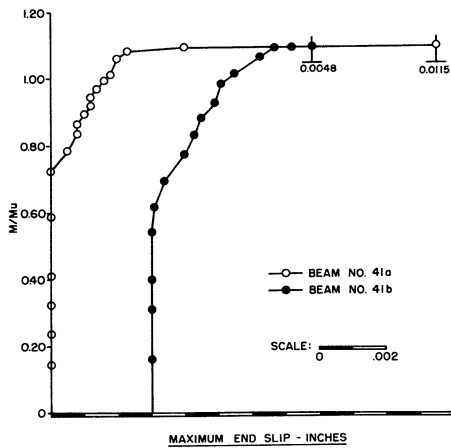


Fig. 19. Plot of  $M/M_u$  vs. maximum end slip for Series 4

The deflections and slips, plotted in Figs. 18 and 19 as functions of  $M/M_u$ , show that the two specimens responded to loading in essentially the same manner until the ultimate load was reached. There was no slip and the load deflection curve was linear beyond the working load level. After the first end slip occurred, the slip continued to increase in both specimens at about the same rate until the moment slip curve leveled off at ultimate load. From then on the two beams responded differently.

In Beam 41a the slip continued to increase without appreciable change in the load and herringbone cracking developed on the top surface of the slab (Fig. 20), indicating failure by shear in the concrete. The test was stopped when the beam refused to carry additional load, soon after the maximum moment was reached.

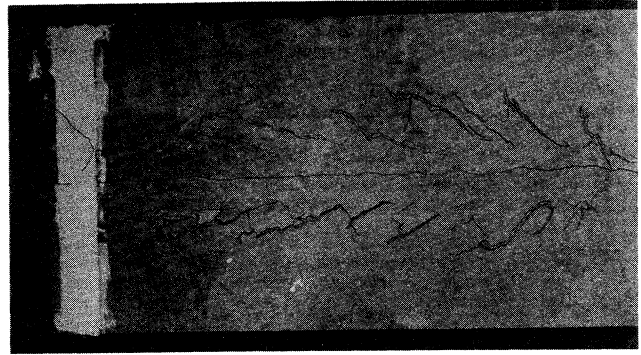


Fig. 20. Top view of slab in Beam 41a, showing the herringbone cracking in the concrete. Such cracking did not prevent the beam from surpassing its calculated capacity.

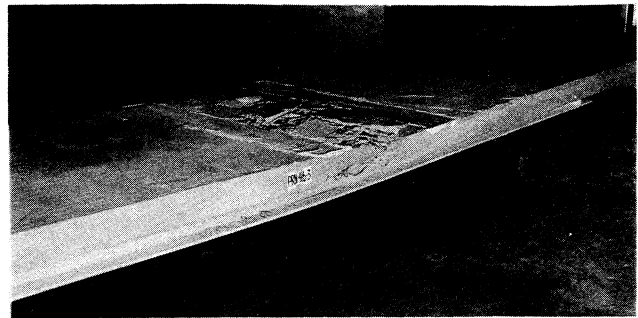


Fig. 21. View of Beam 41b. Note the absence of herringbone type cracking in this beam. Collapse was due to flexural failure (crushing of concrete slab).

Beam 41b failed in flexure at a very small end slip. Figure 21 shows the crushing of the slab in this beam. The post-failure behavior of Beam 41b was remarkably good. The steel section and the remainder of the slab were able to maintain a load considerably in excess of the capacity of the steel section alone.

The difference in the failure of the two specimens would suggest that the design represented a balance between a flexural failure and a failure by shear in the slab. However, some evidence suggests that the mode of failure of Beam 41a may have been caused by faulty testing techniques.

Both beams failed at moments in excess of the theoretical ultimate moment  $M_u$  (Table 3).

The data for Beams 41a, 41b, 11 and 21 illustrate the well known fact that the unsymmetrical steel section is particularly efficient for composite beams. The four beams had the same steel area and were made of the same steel. The moment deflection curves, shown in Fig. 22, show clearly that the symmetrical section was the least efficient while the inverted T section was the most efficient. Series 4 beams were 44 percent stronger than Beam 21 with the symmetrical steel section.

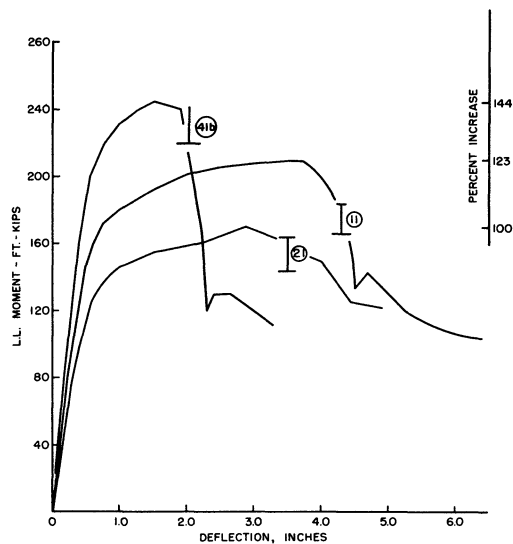


Fig. 22. Comparison of symmetrical and unsymmetrical sections of A36 steel

### CONCLUSIONS

Based on the results of this investigation, which was of an exploratory nature, the following conclusions are tentatively drawn:

1. The use of the hybrid steel sections in composite beams was shown to be feasible. The hybrid beams developed the calculated full plastic strength  $M_u$ . However, their rotation capacity (toughness) was somewhat smaller than that of the composite beams with A36 steel sections.
2. Except for increased strength, there was no significant benefit derived from the high strength webs in the hybrid composite beams.
3. Steel sections without top flanges made very efficient composite beams. Because only two tests were made and differences were observed in the mode of failure of the two beams, further studies of this type of beam are desirable.
4. The floor plate appeared to be effective in reducing end slip and deflection at working load level. However, except in a specimen with a wider plate, it did not increase materially the ultimate strength of these beams with inadequate shear connection.
5. The AISC provisions for the design of stud shear connectors provided adequate factor of safety against shear failure and insured relatively small slips.
6. The ultimate strength of a  $\frac{1}{2}$ -in. diameter stud in the composite beams was approximately 14.6 kips.

### ACKNOWLEDGMENTS

This investigation was carried out under a research grant from the Committee of Steel Plate Producers of American Iron and Steel Institute and under the supervision of the Joint Engineering Subcommittee of the Committee of Steel Plate Producers and the Committee of Structural Steel Producers. Most of the work reported herein was carried out under the direction of the writer by Mr. J. W. Hall, Jr. The writer expresses his appreciation to Mr. Hall for his excellent performance, initiative and assistance.

The author takes this opportunity to thank Dr. Ivan M. Viest for the technical guidance he provided in his capacity as project supervisor for the Joint Engineering Subcommittee and for his continued interest in this project.

The investigation was carried out in the Materials Laboratory of the Department of Civil Engineering at the University of Texas. Appreciation is expressed to the staff of the laboratory and to the many graduate and undergraduate students who assisted in this project. Thanks are also due for the splendid cooperation and help given by the staff of the Bureau of Engineering Research, College of Engineering.

### REFERENCES

1. American Association of State Highway Officials Standard Specifications for Highway Bridges 7th Edition, Div. I, Sect. 9, 1957.
2. American Institute of Steel Construction Specification for the Design, Fabrication, and Erection of Structural Steel for Buildings New York, N. Y., 1963.
3. Joint ASCE-ACI Committee on Composite Construction Tentative Recommendations for the Design and Construction of Composite Beams and Girders for Buildings *Proceedings ASCE, Structural Division, December, 1960*, pp. 73-92.
4. Culver, C., Zarzeczny, P. J. and Driscoll, G. C. Composite Design for Buildings *Progress Report No. 1, Fritz Engineering Laboratory Report No. 279.2, Lehigh University, June, 1960*.
5. Culver, C., Zarzeczny, P. J. and Driscoll, G. C. Composite Design for Buildings *Progress Report No. 2, Fritz Engineering Laboratory Report No. 279.6, Lehigh University, January, 1961*.
6. Viest, I. M., Fountain, R. S. and Singleton, R. C. Composite Construction in Steel and Concrete *McGraw-Hill Book Company, New York, N. Y. 1958*.
7. Toprac, A. A. and Engler, R. A. Plate Girders with High-Strength Steel Flanges and Carbon Steel Webs, *Proceedings, 1961 National Engineering Conference, American Institute of Steel Construction, New York, N. Y., pp. 83-94*.
8. Toprac, A. A. and Hall, J. W. Strength of Three New Types of Composite Beams *SFRL Report No. 01, Department of Civil Engineering, The University of Texas, December, 1964*.
9. Slutter, R. G. and Driscoll, G. C. Composite Design for Buildings *Progress Report No. 3, Fritz Engineering Laboratory Report No. 279.10, Lehigh University, January, 1962*.